

INTERNATIONAL SOCIETY FOR SOIL MECHANICS AND GEOTECHNICAL ENGINEERING



This paper was downloaded from the Online Library of the International Society for Soil Mechanics and Geotechnical Engineering (ISSMGE). The library is available here:

<https://www.issmge.org/publications/online-library>

This is an open-access database that archives thousands of papers published under the Auspices of the ISSMGE and maintained by the Innovation and Development Committee of ISSMGE.

The paper was published in the proceedings of the 7th International Conference on Earthquake Geotechnical Engineering and was edited by Francesco Silvestri, Nicola Moraci and Susanna Antonielli. The conference was held in Rome, Italy, 17 - 20 June 2019.

Soil amplification response of Mexico City clay in the $M_S7.1$ Puebla, 2017 earthquake

E. Garini & G. Gazetas

National Technical University, Athens, Greece

I. Anastasopoulos

ETH, Zurich, Switzerland

ABSTRACT: Soil response of soft alluvial deposits along Mexico City valley is examined during the 19 September 2017, $M_S7.1$ Puebla earthquake. The seismic event occurred approximately 120km south-east of the capital Mexico City, and the recorded peak ground accelerations were lower than 0.2 g on the top of deep soft deposits. However, substantial damage was inflicted on residential infrastructure with numerous collapses and many victims in Mexico City. Recordings were available in more than 50 stations in Mexico City, including motions on rock and on soft clay profiles. The response spectra amplification ratio is calculated and presented for the most characteristic soil profiles, not only for the $M_S7.1$ Puebla event but also for previous earthquakes with magnitude larger than 7. Site effects are studied in terms of simple one dimensional wave propagation of simplified profiles. The effect of three different $G-\gamma$ and $\xi-\gamma$ curves (Vucetic & Dobry, Darenteli, and elastic) on the overall soil response is investigated. Comparison of the calculated with recorded accelerations is presented as well as their response spectra.

1 INTRODUCTION: THE SEISMOTECTONICS OF MEXICO

Mexico's proximity to a subduction zone makes the country prone to strong earthquakes. In particular, the Cocos Plate is gradually sinking beneath the continental plate of North American, creating at their collision the Middle American Trench (Figure 1). In 1985 Michoacan M_S 8.0 earthquake, which originated in the Middle Atlantic Trench, inflicted almost 20,000 deaths in Mexico City and severe damage to building infrastructure. On the 32nd anniversary of the 1985 earthquake, a M_S 7.1 earthquake struck: the Puebla 2017 event.

2 THE $M_S7.1$ PUEBLA 2017 EQ

The Puebla earthquake occurred at 19 September 2017 at 1:14 p.m. (local time) at a focal depth of 51 km in the Puebla Municipality at a distance of 120 km from the Mexico City. Figure 1 demonstrates the epicenter of the 2017 earthquake. On the contrary to the 1995 event which took place at the subduction zone, the 2017 earthquake was an "intra-plate" type on a moderately dipping normal fault. The human loss inflicted by the Puebla event is 370 victims. More than 40 buildings totally collapsed at the Mexico City and widespread damage observed at the Morelos and Puebla regions.

2.1 *Infrastructure damage*

Damage surveys by GEER and ATC reconnaissance teams revealed that most of the collapsed buildings in Mexico City had been erected in 1960s and 1970s with unreinforced masonry

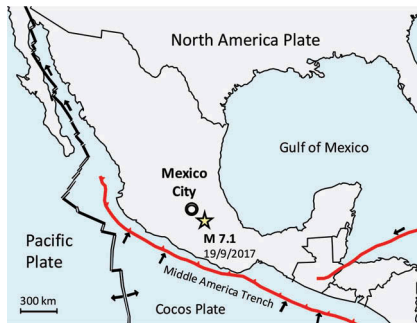


Figure 1. Map of the tectonic plates in the vicinity of Mexico. With star is marked the epicenter of the 2017 EQ.



Figure 2. The Osa Mayor rocking failure: (a) plan view of the 15-floor RC double L-shaped building, (b) the opening between the two L-buildings as seen from the 11th floor, and (c) detail of the uplifted corner (with the turquoise double end arrow is noted the horizontal gap induced by the rocking motion of the building).

walls confined by non-ductile concrete frames. Two general types of building failures are observed. Structurally driven damages: soft floors, pancake collapses, short columns, pounding; and soil driven failures: foundation rocking leading to permanent rotation. The last soil-driven type of failure is of more interest to us, as it is a consequence of the soft Mexico City clay presence and the SSI effects.

For example, in Figure 2 is pictured a 15-story residential building at Osa Mayor neighborhood, constructed during 1970s and consisting by two L-shaped buildings connected at their corners through the staircase and elevator shaft. The building lays on top of a 80 meter soft clay deposit, and its foundation consists of a mat RC slab with friction piles. Severe damage was inflicted to the structure during the Puebla earthquake, leading to the permanent evacuation of it. Apart from the local structural damage at every floor, total separation along the staircase was induced by the rocking motion of the right L-shaped building. The response of the structure and its subsequent damage was dominated by the 80 m soft clay seismic response and interaction.

2.2 Ground motions

CIRES (Centro de Instrumentación y Registro Sísmico) strong motion network had installed about 78 accelerograph devices in Mexico City. Seven of them (those with the strongest recordings from the 2017 Puebla EQ) are chosen as indicative of the seismic severity of the earthquake. Their elastic response spectra are portrayed in Figure 3.

As can be seen from Figure 3, the maximum values recorded on the ground are under 0.2 g. Nevertheless, the spectral values exceed 0.5 g for a wide range of periods, confirming the motions' destructive potential.

3 THE SCT AND CAO SITES

Mexico City is located on top of a volcanic plateau surrounded by volcanic mountains. Figure 4 is a crude geologic map of Mexico City, presenting the three geological zones and the location of the accelerograph stations that are studied here. The Lake Zone consists by

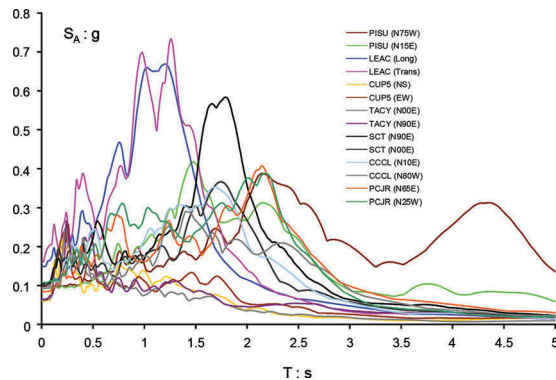


Figure 3. Acceleration response spectra of the horizontal components of ground motions recorded at seven stations of Mexico City during the 2017 Puebla earthquake.

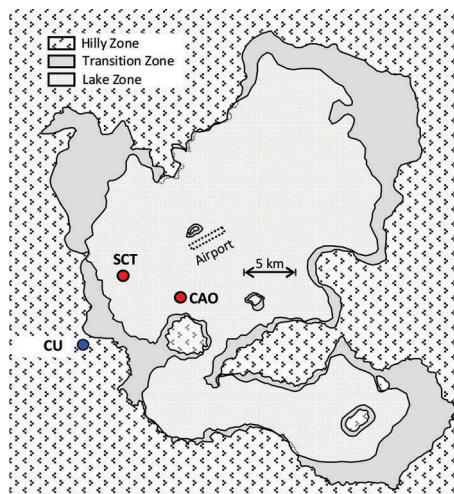


Figure 4. Geologic map of Mexico City and locations of the three stations studied in the article.

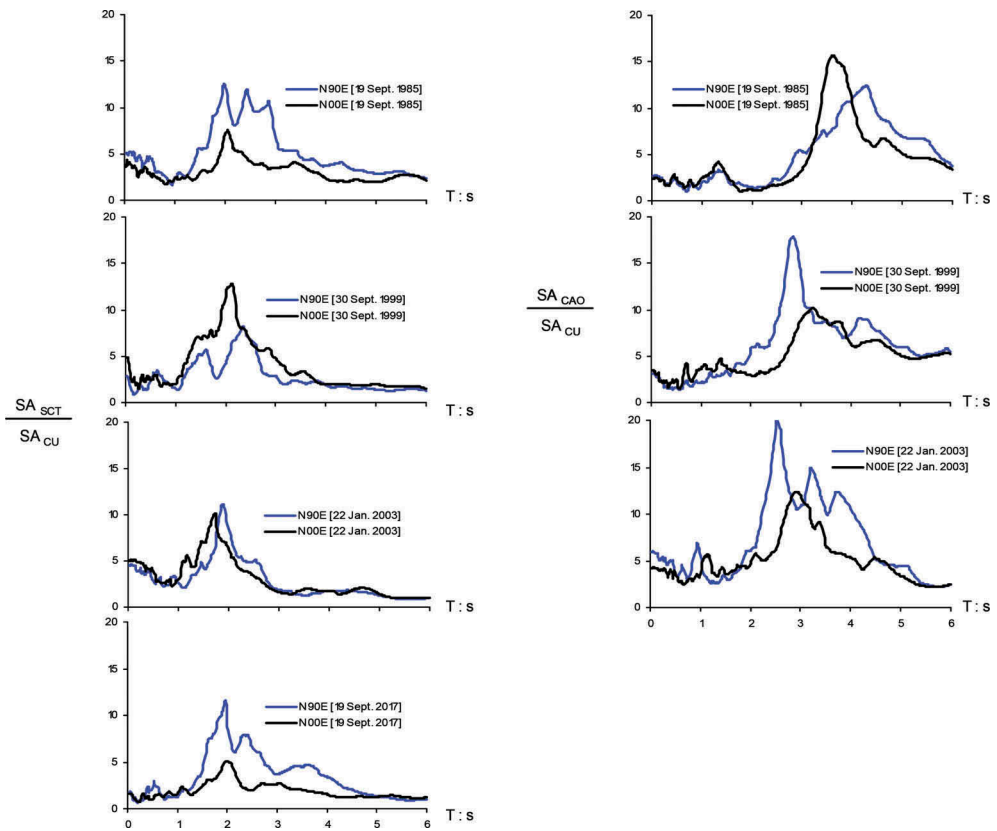


Figure 5. Amplification ratio of the SCT (left) and CAO (right) response spectra over the CU spectra. The CAO station stopped its operation in 2010, therefore there was no recording for the 2017 event.

lacustrine clay, which is extremely deformable. The Hilly Zone consists of basaltic and andesitic lava whereas the Transition Zone lies between the Hilly and Lake Zones with clay lower than 20 m.

CU is located in the Hilly Zone of the city, and as a rock-outcrop station its recording is employed as excitation at the base of our models. SCT and CAO stations rest on the Lake Zone at a 40 m and 60 m thick clay deposit respectively. With the assumption of a mean shear wave velocity $V_s = 80$ m/s for the Mexico City clay, the fundamental periods of these deposits are estimated to be 2 seconds for the SCT and 3.5-4 seconds for the CAO sites. To this end, Figure 5 depicts the amplification ratio of the recorded SCT and CAO motions for the seismic events of Table 1 with respect to the CU rock motions. It is evident for all earthquake cases,

Table 1. List of earthquakes with magnitude larger than 7, which studied herein.

Earthquake Name	Date	Magnitude
Michoacan	19 Sept.1985	8.0
Oaxaca	30 Sept. 1999	7.4
Colima	22 Jan.2003	7.5
Puebla	19 Sept. 2017	7.1

that the period in which the maximum amplification occurs is in fully agreement with our estimation.

4 SOIL AMPLIFICATION ANALYSES

The 1D analysis of the SCT and CAO site responses is performed analytically (with SHAKE, Schnabel et al. 1972) using CU records as rock-outcrop excitation. Figure 6 presents the simplified soil profiles analysing herein. For both of them, the mean average shear-wave velocity is taken equal to 80 m/s, and the specific soil's weight 12 kN/m³. The dynamic properties of Mexico City's clay is described by the G- γ , ξ - γ curves of: Vucetic & Dobry (1987) for plasticity indices PI = 100 and PI = 200, and Darendeli (2001) for plasticity index PI = 100 and mean effective stress $\sigma'_o = 25$ kPa.

Acceleration response spectrum on the ground surface of the SCT is compared in Figure 7(b) with the spectrum of the N90E horizontal component of the 2017 record. Also, the detailed acceleration time histories are compared in Figure 7(a). The peak acceleration value is captured along with the first part of the signal (for $t < 45$ s). However, for $t > 45$ s, 1D analysis does not reproduce adequately the real record. In terms of the response spectra, soil amplification analysis approximates quite well the real one; at the frequency region of $1.5 \text{ s} < T < 2.5 \text{ s}$, analysis underestimates the spectral response.

4.1.1 Influence of G- γ and ξ - γ curves

The sensitivity of soil response to the employed G- γ , ξ - γ curves is shown in Figures 8 and 9 for the SCT and CAO sites, respectively. In Figure 8, the presented record belong to the M_S 8.0, 1985 Michoacan earthquake. In case of the SCT site, as can be seen in Figure 8, the effect of plasticity index on soil's response is not prominent. The only differences are noted in the vicinity of the peak: spectral response for PI = 200 exceeds slightly that for PI = 100. The explanation is straight-forward: the larger the plasticity index, the more elastic the soil becomes. Thus, for the same level of shear strain, the reduction of shear modulus is smaller and the same is true for the increase of damping.

For the case of CAO site, the influence of G- γ , ξ - γ curves is significant as can be seen in Figure 9 for the M_W 7.4, 1999 Oaxaca earthquake. Notice, that the elastic response (no reduction of G, constant damping of 3%) leads to better results than the induced spectrum using the Darendeli (PI = 100, $\sigma'_o = 25$ kPa) or the Vucetic and Dobry (PI = 200) curves. The reason is the almost elastic behaviour of the Mexico City clay, as we mention before for the SCT site.

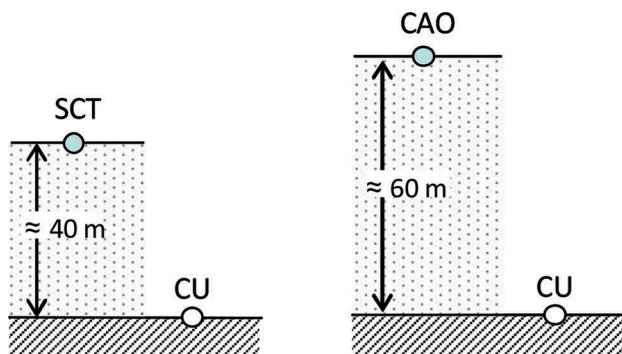


Figure 6. Sketches of the simplified soil profiles of the SCT and CAO sites (after Romo & Seed, 1987).

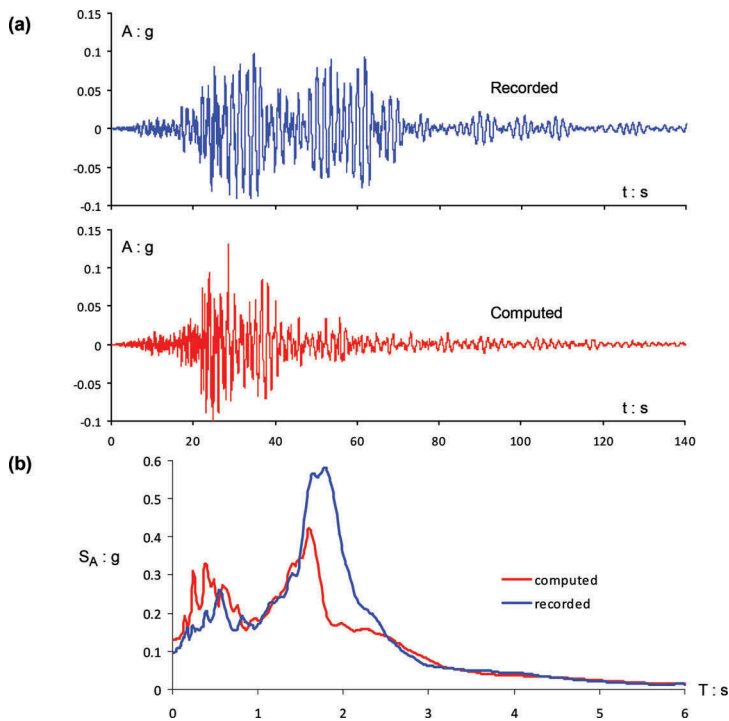


Figure 7. Comparison of the computed (red line) and recorded (blue) SCT response in terms of: (a) detailed acceleration time histories and (b) response spectra, for the 2017 earthquake. [utilised the Vucetic & Dobry 1987 curves for $PI = 100$].

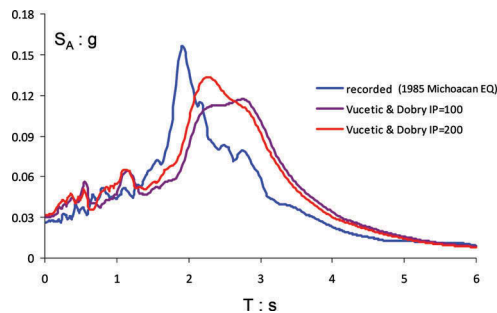


Figure 8. Comparison of the 1985 Michoacan earthquake SCT-N00E component response spectrum (blue line) with the computed response spectra obtained by utilising the Vucetic & Dobry curves with $PI = 100$ (dark red) and $PI = 200$ (red).

5 CONCLUSION

One-dimensional wave propagation analysis can explain adequately both the resonant period and the resonant spectral value, of Mexico City clay's response, at least for the two presented locations of SCT and CAO stations. Nonetheless, several other phenomena than the propagation of vertical shear waves might be substantial in order to fully capture Mexico City clay's response. For instance, the topography of Mexico Valley (Bard & Bouchon, 1995) and the

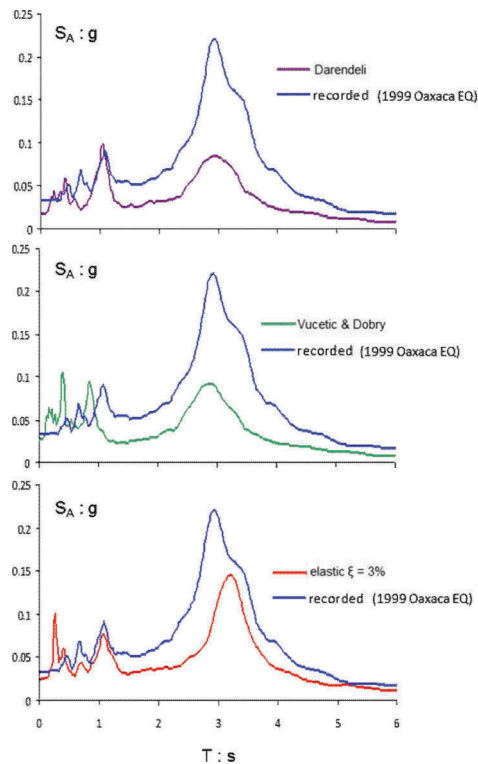


Figure 9. Comparison of the 1999 Oaxaca earthquake CAO-N90E component response spectrum (blue line) with the computed response spectra obtained by utilising: the Darendeli (purple), Vucetic & Dobry (green) curves and the elastic response (red) as well.

soil-structure interaction (Celebi, 2007), among others. Special attention should be paid in the G - γ , ξ - γ curves utilised to describe the dynamic properties of the soil, as Mexico's clay demonstrates a unique seismic behaviour.

REFERENCES

- Anderson, J.G., Bodin, P., Brune, J., Prince, J., Singh, S., Quaa, R., Onate, M., Mena, E. 1986. Strong ground motion and source mechanism of the Mexico earthquake of September 19, 1985, *Science* 233: 1043–1049.
- Auvinet, G., Moises, J. 2011. Geotechnical characterization of Mexico City subsoil, *Proceedings of the 2011 Pan-Am CGS Geotechnical Conference*, October 2–6, Toronto, Ontario, Canada.
- Bard, P.Y., Bouchon, M. 1995. The two-dimensional resonance of sediment-filled valleys, *Bulletin of the Seismological Society of America* 75: 519–541.
- Celebi, M. 2007. Beating effect identified from seismic responses of instrumented buildings, *Proceedings of Structures Congress*, doi:10.1061/40946(248)14.
- Darendeli, M.B., Stokoe, K.H. 2001. Development of a new family of normalized modulus reduction and material damping curves, *Geotechnical Engineering Report GD01-1*, University of Texas at Austin, Austin.
- Dobry, R., Vucetic, M. 1987. Dynamic properties and seismic response of soft clay deposits. *Proceedings of Simposio Internacional de Ingeniería Geotécnica de Suelos Blandos*, M. J. Mendoza (editor), México, Sociedad Mexicana de Mecánica de Suelos, 2: 49–85.
- Mayoral, J.M., Romo, M.P., Osorio, L. 2008. Seismic parameters characterization at Texcoco lake, Mexico, *Soil Dynamics and Earthquake Engineering* 28(7): 507–521.

- Ovando-Shelley, E., Romo, M.P., Ossa, A. 2007. The sinking of Mexico city: Its effects on soil properties and seismic response, *Soil Dynamics and Earthquake Engineering* 27: 333–343.
- Paolucci, R. 1993. Soil-structure interaction effects on an instrumented building in Mexico City, *European Earthquake Engineering VII* (3): 33–44.
- Romo, M.P., Seed, H.B. 1986. Analytical Modeling of Dynamic Soil Response in the Mexico Earthquake of September 19, 1985. *Proceedings of the International Conference on the Mexico Earthquakes-1985*, Mexico City, Mexico, 148–162.
- Schnabel, P.B., Lysmer, J., Seed, H.B. 1972. SHAKE: A Computer Program for Earthquake Response Analysis of Horizontally Layered Sites, Report No. EERC 72–12, EERC, University of California, Berkeley, California